

## A study on Si and P doped h-BN sheets: DFT calculations

Hatice KÖKTEN\*, Şakir ERKOÇ

Department of Physics, Middle East Technical University, Ankara, Turkey

Received: 26.06.2014 • Accepted: 16.08.2014 • Published Online: 10.11.2014 • Printed: 28.11.2014

**Abstract:** Structural properties and energetics of silicon and phosphorus doped hexagonal boron nitride sheets were investigated by performing density functional theory calculations. The dopant atoms were substituted in a neutral charge state at either the B or the N site in the system as an impurity. All the systems under consideration were fully optimized. A systematic study was performed to see the effect of cell size on the calculated quantities, such as bond length, charge transfer, and defect formation energies. It was found that both silicon and phosphorus atom substitutions cause the bond lengths to increase with respect to the pristine sheets. Si atom replaced on the N site yields relatively large charge transfer from Si to the lattice. Substitutions of Si at the B site and of P at the N site are exothermic processes, while for the other cases the processes are endothermic.

**Key words:** h-BN sheet, density functional theory, point defects

### 1. Introduction

Boron nitride (BN), a III-nitride, is a material with technological importance. The BN crystal has several polymorphous forms: cubic boron nitride (c-BN), wurtzite boron nitride (w-BN), rhombohedral BN (r-BN), and hexagonal BN (h-BN). BN has many fascinating properties. It is as hard as diamond, with w-BN being even harder than diamond [1], it has a wide band gap [2], it is a remarkable thermal and chemical stabilizer [3], it has good thermal conductivity, and it has high mechanical strength; furthermore, it is a corrosion and oxidation resistant material. These properties make it an important material for many applications. h-BN was synthesized at atmospheric pressure by Kubota et al. [4] as a promising deep-ultraviolet-light emitter. It is a suitable material for producing nanotubes [5], hydrogen storage [6], neutron detectors [7], and other technological applications.

In recent years, h-BN (monolayer, 2-dimensional honeycomb structure), a III-V compound of boron and nitrogen with strong covalent  $sp^2$  bonds, has gained great interest as a two-dimensional (2D) material, following the isolation of graphene from graphite by Novoselov et al. [8]. The h-BN monolayer, which is a single 2-dimensional sheet similar to graphene, has very different electronic characteristics. This material has been studied extensively both experimentally [9–18] and theoretically [19–21]. h-BN is a material with a wide gap with important applications for optoelectronic technologies [22,23]. It has been also shown that this material enhances the performance of graphene-based electronic devices [24–27] and other technological applications [28]. Moreover, as stated in Ref. [29] 'the oxidation resistance of h-BN nanosheets makes them more preferable for high-temperature applications than graphene'.

\*Correspondence: [kokten@metu.edu.tr](mailto:kokten@metu.edu.tr)

The h-BN sheet can be grown using different techniques such as chemical vapor deposition (CVD) [30,31], liquid-phase exfoliation [32], and controllable electron beam radiation [33]. Feng et al. [34] obtained a few atomic layer h-BN sheets using a pulsed laser deposition technique (CO2-PLD). Initially, Corso et al. [30] synthesized a self-assembled superstructure of h-BN monolayers on a Rh(111) surface. Their discovery has accelerated investigations on the growth of h-BN monolayers of many transition metal surfaces from various aspects [35–39].

Doping and native defects affect the electronic, optical, chemical, and magnetic properties of the materials. In a previous theoretical study [40], the electronic and magnetic properties of both  $V_B$  and  $V_N$  monovacancies in the h-BN sheet were investigated. Du et al. [41] found that  $V_B$  has a lower formation energy than  $V_N$  and these lattice defects in the h-BN sheet have been identified experimentally by Jin et al. [13]. Theoretically, different defects in the h-BN sheet have been studied and their formation energies have been calculated [42]. The carbon (C) atom is the most common dopant for the h-BN sheet. It can provide n- and p-doping [43,44]. The doping of silicon (Si), which belongs to the same group as C, is also studied for carbon nanotubes (CNTs) [45] and boron nitride nanotubes (BNNTs) [46]. In the present work, Si and phosphorus (P) substituted h-BN sheets were considered using density functional theory (DFT) in order to assess the influence of Si and P dopants on the structural and energetics properties at the B and N sites.

## 2. Computational methods

The CRYSTAL03 package program [47] was used in the present work, in which the DFT formalisms are implemented. CRYSTAL03 uses the localized Gaussian-type basis sets: the 6-21 $G^*$  basis set has been used for B and N atoms. The basis sets 88-31 $G^*$  and 85-21d1G are used for Si and P atoms, respectively. The experimental values of bulk lattice parameters ( $a = 2.50399 \text{ \AA}$  and  $c = 6.6612 \text{ \AA}$ ) were used [48]. CRYSTAL03 computes the matrix elements of the coulomb and exchange terms by direct summation of infinite periodic lattice. The reciprocal space integration was performed by sampling the Brillouin zone of the unit cells with the  $8 \times 8 \times 1$  and  $8 \times 16 \times 1$  Monkhorst–Pack net [49], which provides the balanced summation in direct and reciprocal spaces [50]. To ensure the numerical convergence of the self-consistent-field procedure the numerical threshold was set to  $10^{-9}$  a.u. for the total energy.

Si and P doped h-BN sheets were investigated by performing DFT calculations using the B3LYP hybrid functional [51,52]. A full geometry optimization and the energetic calculations were carried out. One B or N atom is replaced with one Si or P atom to create the doping atom ( $Si_B$ ,  $Si_N$ ,  $P_B$ , and  $P_N$ ). To evaluate the relative stability of Si and P doping in the h-BN sheet with respect to the pristine h-BN sheet, the formation energies were obtained from the relation

$$E_f(X) = E_d + E(B \text{ or } N) - E_p - E(X) \quad (1)$$

where  $E_d$  is the energy of the defective system,  $E_p$  is the energy of the perfect system, and  $E(B \text{ or } N)$  is the energy of the isolated boron or nitrogen atom, whereas  $E(X)$  is the energy of the isolated dopant atom (Si or P). To be able to see the size effect on the calculated quantities, different unit cell sizes were considered, such as  $5 \times 5$ ,  $6 \times 6$ ,  $7 \times 7$ ,  $8 \times 8$ , and  $9 \times 9$ . The corresponding total numbers of atoms for these models are 50, 72, 98, 128, and 162.

### 3. Results and discussion

We tried several working cell sizes to see the convergence in the calculated quantities, which are tabulated in Tables 1–3 with respect to working cell size. A sample picture for optimized pristine and P substituted models generated from the 5 x 5 working cell is displayed in Figure. Some of the calculated quantities show a smooth convergence; however, some of them show slight fluctuations. Bond lengths show a smooth increase with respect to cell size in both cases, Si and P doped models. On the other hand, the amounts of excess charge on the atoms do not show a dependence on cell size.

**Table 1.** Si doped h-BN sheet: the bond length (d, in Å) and charge transferred ( $|e|$ ).

Model	$d(Si_B)$	$d(Si_N)$	Charge( $Si_B$ )	Charge( $Si_N$ )
5X5	1.645	1.748	0.286	0.459
6X6	1.648	1.754	0.287	0.457
7X7	1.650	1.757	0.287	0.457
8X8	1.651	1.759	0.287	0.457
9X9	1.653	1.761	0.286	0.456

**Table 2.** P doped h-BN sheet: the bond length (d, in Å) and charge transferred ( $|e|$ ).

Model	$d(P_B)$	$d(P_N)$	Charge( $P_B$ )	Charge( $P_N$ )
5X5	1.644	1.711	0.222	0.375
6X6	1.647	1.716	0.222	0.375
7X7	1.649	1.718	0.222	0.374
8X8	1.650	1.720	0.222	0.374
9X9	1.651	1.721	0.222	0.374

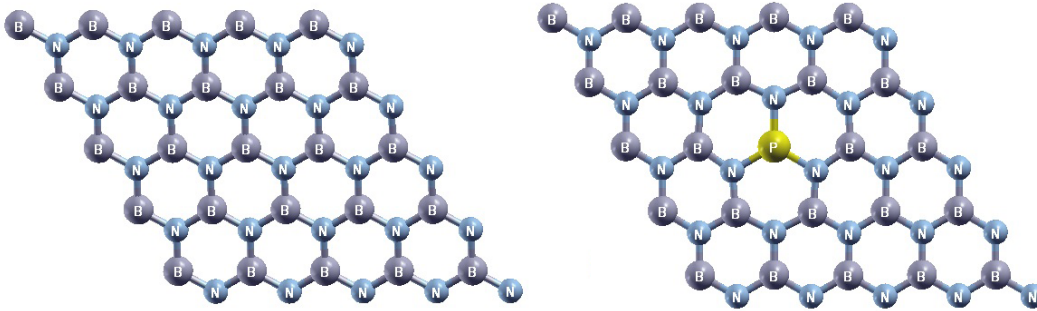


**Figure.** Optimized 5 x 5 h-BN monolayer working cells for (a) pristine and (b) P substituted ( $P_B$ ) models.

The structural changes caused by the substitution atoms are significant. The optimized bond length of B-N (1.446 Å) for the pristine structure is in good agreement with experimental values of 1.44 Å [53], as expected (because the lattice was constructed by using the experimental data). The bond lengths of the doped h-BN and the charge transfers from Si and P atoms to the h-BN layer are given in Tables 1 and 2. There is an extension of bond length as a result of doping with both Si and P atoms. In the Si doping at B site the Si-N bond length expands about 14.3% with respect to the pristine case; on the other hand, at the N site the Si-B

bond length expands about 21.6%. In the case of P doping related with bond lengths, similar behavior appears as in the Si doping case. According to the results presented in Tables 1 and 2 the bond lengths can be ordered as the following: P-N < Si-N < P-B < Si-B. On the other hand, charge transfer from the substituent atoms to the h-BN sheet show an interesting feature. The Si atom loses more electrons with respect to the P atom. The largest charge transfer takes place on  $Si_N$ , whereas the smallest charge transfer takes place on  $P_B$ .

The calculated formation energies for  $Si_B$ ,  $Si_N$ ,  $P_B$ , and  $P_N$  impurities are given in Table 3. According to the calculated formation energy values, the processes of Si doping at the B site and P doping at the N site are exothermic, whereas the processes of Si doping at the N site and P doping at the B site are endothermic. All energy values show a smooth convergence with respect to the cell size. The chemical doping with  $Si_B$  and/or  $P_N$  is expected to be easier than that of  $Si_N$  and/or  $P_B$ . In particular,  $Si_B$  has a larger negative formation energy with respect to the other cases. The present results agree with recent experimental findings [54,55] and a previous DFT calculation [56].

**Table 3.** Defect formation (relaxed  $E_f$ ) energies (in eV) of h-BN sheet.

Model	Atomic % of doping	$E_f$ $Si_B$	$E_f$ $Si_N$	$E_f$ $P_B$	$E_f$ $P_N$
5X5	2.000	-3.419	1.093	1.153	-1.146
6X6	1.388	-3.480	0.927	1.103	-1.255
7X7	1.020	-3.513	0.833	1.075	-1.316
8X8	0.781	-3.533	0.777	1.058	-1.353
9X9	0.618	-3.547	0.740	1.047	-1.378

## References

- [1] Pan, Z.; Sun, H.; Zhang, Y.; Chen, C. *Phys. Rev. Lett.* **2009**, *102*, 055503.
- [2] Arnaud, B.; Lebegue, S.; Rabiller, P.; Alouani, M. *Phys. Rev. Lett.* **2006**, *96*, 026402.
- [3] Han, W.-Q.; Mickelson, W.; Cumings, J.; Zettl, A. *Appl. Phys. Lett.* **2008**, *93*, 1110–1114.
- [4] Kubota, Y.; Watanabe, K.; Tsuda, O.; Taniguchi, T. *Science* **2007**, *317*, 932–934.
- [5] Ma, R.; Bando, Y.; Sato, T.; Kurashina, K. *Chem. Mater.* **2001**, *13*, 2965–2971.
- [6] Wang, P.; Orimo S.; Matsushima, T.; Fujii, H. *Appl. Phys. Lett.* **2002**, *80*, 318–320.
- [7] Li, J.; Dahal, R.; Majety, S.; Lin, J. Y.; Jiang, H. X. *Nucl. Instr. and Meth. A* **2011**, *654*, 417–420.
- [8] Novoselov, K. S.; Geim, A. K.; Morozov, S. V.; Jiang, D.; Zhang, Y.; Dubonos, S. V.; Grigorieva, I. V.; Firsov, A.A. *Science* **2004**, *306*, 666–669.
- [9] Pacile, D.; Meyer, J. C.; Girit, C. O.; Zettl, A. *Appl. Phys. Lett.* **2008**, *92*, 133107.
- [10] Han, W. Q.; Wu, L.; Zhu, Y.; Watanabe, K.; Taniguchi, T. *Appl. Phys. Lett.* **2008**, *93*, 223103.
- [11] Meyer, J. C.; Chuvilin, A.; Algara-Siller, G.; Biskupek, J.; Kaiser, U. *Nano Lett.* **2009**, *93*, 2683–2689.
- [12] Warner, J. H.; Rummeli, M. H.; Bachmatiuk, A.; Buchner, B. *ACS Nano* **2010**, *4*, 1299–1304.
- [13] Jin, C.; Lin, F.; Suenaga, K.; Iijima, S. *Phys. Rev. Lett.* **2009**, *102*, 195505.
- [14] Alem, N.; Erni, R.; Kisielowski, C.; Rossell, M. D.; Gannett, W.; Zettl, A. *Phys. Rev. B* **2009**, *80*, 155425.
- [15] Song, L.; Ci, L.; Lu, H.; Sorokin, P. B.; Jin, C.; Ni, J.; Kvashnin, D. G.; Lou, J.; Yakobson, B. I.; Ajayan, P. M. *Nano Lett.* **2010**, *10*, 3209–3215.

- [16] Lin, Y.; Williams, T. V.; Xu, T-B.; Cao, W.; Elsayed-Ali, H. E.; Connell, J. W. *J. Phys. Chem. C* **2011**, *115*, 2679–2685.
- [17] Gao, Y.; Ren, W.; Ma, T.; Liu, Z.; Zhang, Y.; Liu, W-B.; Ma, L-P.; Ma, X.; Cheng, H-M.; *ACS Nano* **2013**, *7*, 5199–5206.
- [18] Hemmi, A.; Bernard, C.; Cun, H.; Roth, S.; Klockner, M.; Kalin, T.; Weinl, M.; Gsell, S.; Schreck, M.; Osterwalder, J.; Greber, T. *Rev. Scient. Inst.* **2014**, *85*, 035101.
- [19] Golberg, D.; Bando, Y.; Huang, Y.; Terao, T.; Mitome, M.; Tang, C.; Zhi, C. *ACS Nano* **2010**, *4*, 2979–2993.
- [20] Yang, W.; Yang, Y.; Zheng, F.; Zhang, P. *J. Chem. Phys.* **2013**, *139*, 214708.
- [21] Singh, S. K.; Neek-Amal, M.; Costamagna, S.; Peeters, F. M. *Phys. Rev. B* **2013**, *87*, 184106.
- [22] Watanabe, K.; Taniguchi, T.; Kanda H. *Nat. Mater.* **2004**, *3*, 404–409.
- [23] Li, L. H.; Chen, Y.; Cheng, B. M.; Lin, M. Y.; Chou, S. L.; Peng, Y. C. *Appl. Phys. Lett.* **2012**, *100*, 141104.
- [24] Slavinska, J.; Zasada, I.; Kosinski, P.; Klusek, Z. *Phys. Rev. B* **2010**, *82*, 085431.
- [25] Dean, C. R.; Young, A. F.; Meric, I.; Lee, C.; Wang, L.; Sorpenfrei, S.; Watanabe, K.; Taniguchi, T.; Kim, P.; Shepard K. L.; Hone, J. *Nat. Nanotech.* **2010**, *5*, 722–726.
- [26] Wang, H.; Taychatanapat, T.; Hsu, A.; Watanabe, K.; Taniguchi, T.; Jarillo-Herrero, P.; Palacios, T. *Electron Device Lett.* **2011**, *32*, 1209–1211.
- [27] Lee, K. H.; Shin, H.-J.; Lee, J.; Lee, I.-Y.; Kim, G.-H.; Choi, J.-Y.; Kim S.-W. *Nano Lett.* **2012**, *12*, 714–718.
- [28] Das, S.; Kim, M.; Lee, J-W.; Choi, W. *Critical Rev. in Solid State and Mater. Science* **2014**, *39*, 231–254.
- [29] Li, L. H.; Cervenka, J.; Watanabe, K.; Taniguchi, T.; Chen, Y. *ACS Nano* **2014**, *8*, 1457–1462.
- [30] Corso, M.; Auwarter, W.; Muntwiler, M.; Tamai, A.; Greber, T.; Osterwalder, J. *Science* **2004**, *303*, 217–220.
- [31] Shi, Y.; Hamsen, C.; Jia, X.; Kim, K. K.; Reina, A.; Hofmann, M.; Hsu, A. L.; Zhang, K.; Li, H.; Juang, Z.-Y.; Dresselhaus, M. S.; Li, L.-J.; Kong, J. *Nano Lett.* **2010**, *10*, 4134–4139.
- [32] Coleman, J. N.; Lotya, M.; O’Neil, A.; Bergin, S. D.; King, P. J.; Khan, U.; Young, K.; Gaucher, A.; Sukanta, D.; Smith, R. J. *Science* **2011**, *331*, 568–571.
- [33] Novoselov, K. S.; Jiang, D.; Schedin, F.; Booth, T. J.; Khotkevich V. V.; Morozov, S. V.; Geim, A. K. *Proc. Nat. Acad. Sci. USA* **2005**, *102*, 10451–10453.
- [34] Feng, P.X.; Sajjad, M. *Materials Lett.* **2012**, *89*, 206–208.
- [35] Muller, F.; Stowe K.; Sachdev, H. *Chem. Mater.* **2005**, *17*, 3464–3467.
- [36] Morscher, M.; Corso, M.; Greber T.; Osterwalder, J. *Surf. Sci.* **2006**, *600*, 3280–3284.
- [37] Orlandi, F.; Larciprete, R.; Lacovig, P.; Boscarato, I.; Baraldi, A.; Lizzit, S. *J. Phys. Chem. C* **2012**, *116*, 157–164.
- [38] Gao, Y.; Ren, W.; Ma, T.; Liu, Z.; Zhang, Y.; Liu, W.-B.; Ma, L.-P.; Ma, X.; H.-M. Cheng, H.-M. *ACS Nano* **2013**, *7*, 5199–5206.
- [39] Ohtomo, M.; Yamauchi, Y.; Kuzubov, A. A.; Eliseeva, N. S.; Avramov, P. V.; Entani, S.; Matsumoto, Y.; Naramoto, H.; Sakai, S. *App. Phys. Lett.* **2014**, *104*, 051604.
- [40] Si, M. S.; Xue, D. S. *Phys. Rev. B* **2007**, *75*, 193409.
- [41] Du, A.; Chen, Y.; Zhu, Z.; Amal, R.; Lu, G. Q. (Max).; Smith, S. J. *J. Am. Chem. Soc.* **2009**, *131*, 17354–17359.
- [42] Shevlin, S. A.; Guo, Z. X. *Phys. Rev. B* **2007**, *76*, 024104.
- [43] Berseneva, N.; Krasheninnikov, A. V.; Nieminen, R. M. *Phys. Rev. Lett.* **2011**, *107*, 035501.
- [44] Park, H.; Wadehra, A.; Wilkins, J. W.; Castro Neto, A. H. *Appl. Phys. Lett.* **2012**, *100*, 253115.
- [45] Avramov, P. V.; Sorokin, P. B.; Fedorov, A. S.; Fedorov, D. G.; Maeda, Y. *Phys. Rev. B* **2006**, *74*, 245417.
- [46] Si, M. S.; Xue, D. S. *Europhys. Lett.* **2006**, *76*, 664–669.

- [47] Saunders, V. R.; Dovesi, R.; Roetti, C.; Zicovich-Wilson, C. M.; Harrison, N. M. CRYSTAL03 User's Manual, Universita di Torino, Torino, **2003**: [www.crystal.unito.it](http://www.crystal.unito.it).
- [48] Lynch, R. W.; Drickamer, H. G. *J. Chem.* **1966**, *44*, 181–184.
- [49] Monkhorst, H. J.; Pack, J. D. *Phys. Rev. B* **1976**, *13*, 5188–5191.
- [50] Bredow, T.; Evarestov, R. A.; Jug, K. *Phys. Stat. Solidi b* **2000**, *222*, 495–514.
- [51] Becke, A. D. *Phys. Rev. A* **1993**, *222*, 3098–3100.
- [52] Lee, C.; Yang, W.; Parr, R. G. *Phys. Rev. B* **1998**, *37*, 785–798.
- [53] Nag, A.; Raidongia, K.; Kailash, P. S.; Hembram, S.; Datta, R.; Waghmare, U. V.; Rao, C. N. R. *ACS Nano* **2010**, *4*, 1539–1544.
- [54] Li, X.; Feng, S.; Liu, X.; Hou, L.; Gao, Y.; Wang, Q.; Liu, N.; Zhang, H.; Chen, Z.; Zheng, J.; et al. *App. Surface Science* **2014**, *308*, 31–37.
- [55] Cho, Y. J.; Kim, C. H.; Kim, H. S.; Park, J.; Choi, H. C.; Shin, H-J.; Gao, G.; Kang, H. S. *Chem. Mater.* **2009**, *21*, 136–143.
- [56] Gupta, S. K.; He, H.; Banyai, D.; Si, M.; Pandey, R.; Karna, S. P. *Nanoscale* **2014**, *6*, 5526–5531.